Available online at www.sciencedirect.com
ScienceDirect
Cement and Concrete Research 37 (2007) 360–368
Cement and Concrete Research

3D experimental investigation of the microstructure of cement pastes using synchrotron X-ray microtomography (μCT)

E. Gallucci [a,*], K. Scrivener [a], A. Groso [b], M. Stampanoni [b], G. Margaritondo [c]

[a] *Laboratory of Construction Materials, Ecole Polytechnique Fédérale de Lausanne, CH-1015 Switzerland*
[b] *Swiss Light Source, Paul Sherrer Institute, CH-5232-Villigen, Switzerland*
[c] *Laboratoire de Spectroscopie Electronique, Ecole Polytechnique Fédérale de Lausanne, CH-1015 Switzerland*

Received 3 May 2005; accepted 23 October 2006

Abstract

Cement pastes aged from 1 to 60 days were studied using synchrotron microtomography on the MS-X04SA beam line at the Swiss Light Source. This allowed three dimensional images to be obtained with a resolution approaching that of backscattered electron images in the SEM. From these images, several features can be extracted and studied, both quantitatively and morphologically. In this study, attention was focused on the reacting anhydrous cement grains and porosity. Three dimensional imaging of capillary porosity allowed the connectivity and tortuosity of the pore network to be studied. It is shown that the degree of connectivity of the pore network is very sensitive to both the spatial resolution of the images and the evolution of contrast resolution during ageing of the cement.

Keywords: D—cement paste; B—microstructure; B—synchrotron microtomography; B—image analysis

1. Introduction

The performance of cement pastes and concretes is controlled by their microstructure, in particular the pore network plays a critical role in determining mechanical properties and interactions with the environment which determine durability. This latter aspect is the focus of considerable research effort. The challenge is to predict the performance of concrete over the lifetime of a structure which is a minimum of several decades and increasingly over a century for the most important structures. For other applications, such as waste disposal, time scales of more than one thousand years must be considered. In order to extrapolate from short term laboratory testing, models of performance must be underpinned by a detailed understanding of the transport mechanisms whereby species from the environment (e.g. Cl^-, SO_4^{2-} ions, CO_2) penetrate into the concrete. In this regard the connectivity of the capillary pore structure is central.

The porosity of cement extends over a wide range of length scales, classically this is divided into:

- so-called 'gel-pores' which are intrinsic to the C-S-H product. This porosity lies in the range of a few nanometres and due to this small size plays only a minor role in transport processes affecting durability and other aspects of performance.
- capillary pores corresponding to the originally water filled spaces not filled by hydration products, the size of these ranges from a few nanometres to tens of micrometers, i.e. more than 4 orders of magnitude,
- air voids, from tens of μm to mm in size are heterogeneities of the original mix. They are a small fraction of the whole porosity and as they are isolated have a minor role on overall transport processes.

The voids in hollow shells or the gaps between unreacted grains and C-S-H shells that are observed in cement pastes may also be considered as porosity although it is not clear to what extent these voids are connected to the capillary pore network [1].

Hence capillary porosity of cement pastes is the main factor affecting the performance of cementitious materials. A large,

* Corresponding author.
E-mail address: emmanuel.gallucci@epfl.ch (E. Gallucci).

0008-8846/$ - see front matter © 2006 Elsevier Ltd. All rights reserved.
doi:10.1016/j.cemconres.2006.10.012

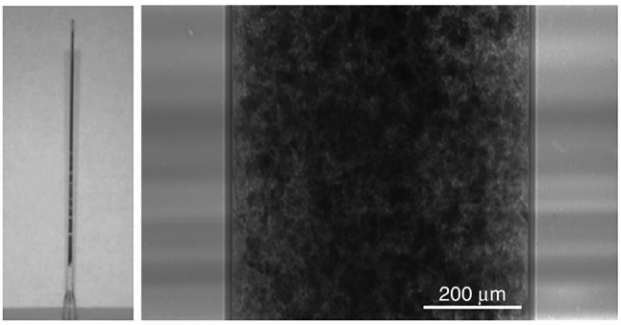

Fig. 1. Sample implementation: picture of the tube filled with cement (left) and synchrotron X-ray transmitted image (right).

extended and connected pore network will be responsible for the ingress of external chemical species into the material which may lead to degradation, whereas porosity consisting of isolated individual pores, even if their total amount is similar, have a less adverse effect on the service life of the material.

Most classical methods for the characterisation of porosity (e.g. Mercury Intrusion Porosimetry), only give information on the overall pore content and threshold pore size but nothing about their real size nor spatial distribution. Over the past decades, modern methods for microstructural characterisation have lead to huge advances in our understanding of the microstructure of cement pastes, and its evolution during hydration. In particular backscattered electron (BSE) images of polished sections in the SEM (e.g. [2]) allow good resolution of the anhydrous and hydrated phases by grey level contrast and can be coupled with chemical information from X-ray spectroscopy. The main shortcoming of the techniques now available is the lack of three dimensional information. While some quantitative parameters, such as overall volume fractions of a phase can be well estimated from 2 dimensional sections, parameters such as connectivity are completely inaccessible. Furthermore, for electron microscopy, cementitious samples must be dried and exposed to high vacuum, which is known to produce irreversible changes in the pores structure, particularly at small sizes. Although comparison with techniques such as environmental electron microscopy indicates that the impact of drying is minimal at the resolution of the backscattered electron technique, the ability to image undried specimens would be a major advantage.

Tomographic methods provide a mean of obtaining images in three dimensions on materials without any prior preparation such as drying [3]. The principle is based on the 3D computed reconstruction of a sample from 2D projections acquired at different angles around its axis of rotation. The higher the number of projections, the higher the resolution of features in the reconstructed volume. Studies on construction materials [4–9] have been performed but were limited to the observation of large scale features (either using low resolution of conventional X-ray tomography (which has now improved to 5 µm) or X-ray synchrotron microtomography). Over the last 10 years there have been some attempts to apply synchrotron microtomography which can attain resolutions of about 1 µm to cement based materials. Bentz et al. reported the first tomographic scans of cement pastes [10,11] made at the ESRF. This facility has also been used by Helfen et al. [12]. Despite these precedents, the exploitation of X-ray microtomography to quantify the microstructural evolution and pore structure of cementitious materials has been modest to date.

As capabilities of microtomography systems in synchrotron radiation facilities have increased, it has now become possible to obtain a complete three dimensional representation with resolution better than 1 µm. The present study concerns the investigation of cement pastes aged between 1 and 60 days: quantitative data from both the solid phases and porosity are reported, the connectivity and percolation of the pore network is qualitatively described and an experimental 3D representation of this network is given for the first time. The dependence between connectivity and resolution is investigated.

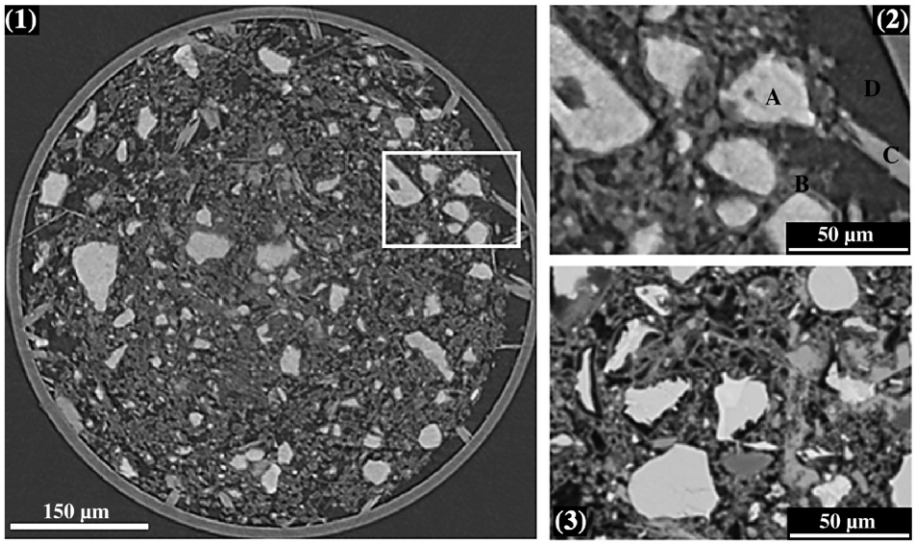

Fig. 2. (1) Reconstructed slice of a 1 day old sample from series 1. (2) zoomed part of rectangle in (1). (3) comparison with similar specimen in SEM. A—unreacted cement grains, B—inner C-S-H, C—calcium hydroxide, D—unfilled spaces (air or water filled porosity).

2. Experimental

2.1. Sample preparation

A CEM I 42.5 Portland cement (OPC) was used for this study. Pastes were prepared at a water to cement ratio W/C of 0.5. This W/C is relatively high for cement paste and equivalent to a concrete W/C of around 0.6 [13]. Cement and distilled water were mixed by hand for 5 min and then injected with a syringe into thin cylindrical glass tubes with a diameter of 600 μm and a wall thickness of 10 μm (Fig. 1). The glass tubes were of Lindemann Glass 14 type (which minimises the scattering of X-rays by the capillary). The use of a thin capillary has significant advantages in reducing the acquisition time for the projections and reducing absorption effects in the centre of the reconstituted sections.

Two series of experiment were conducted with the aim of following the evolution of the hydration process over time. In the first one (called series 1 in this paper), samples were prepared in advance and kept unsealed into water in order to have the desired age at the same date. The samples studied were 1, 3, 7, 14, 28 and 60 days old. This approach was adopted due to the limited access to the synchrotron. As will be seen later, the main drawback of

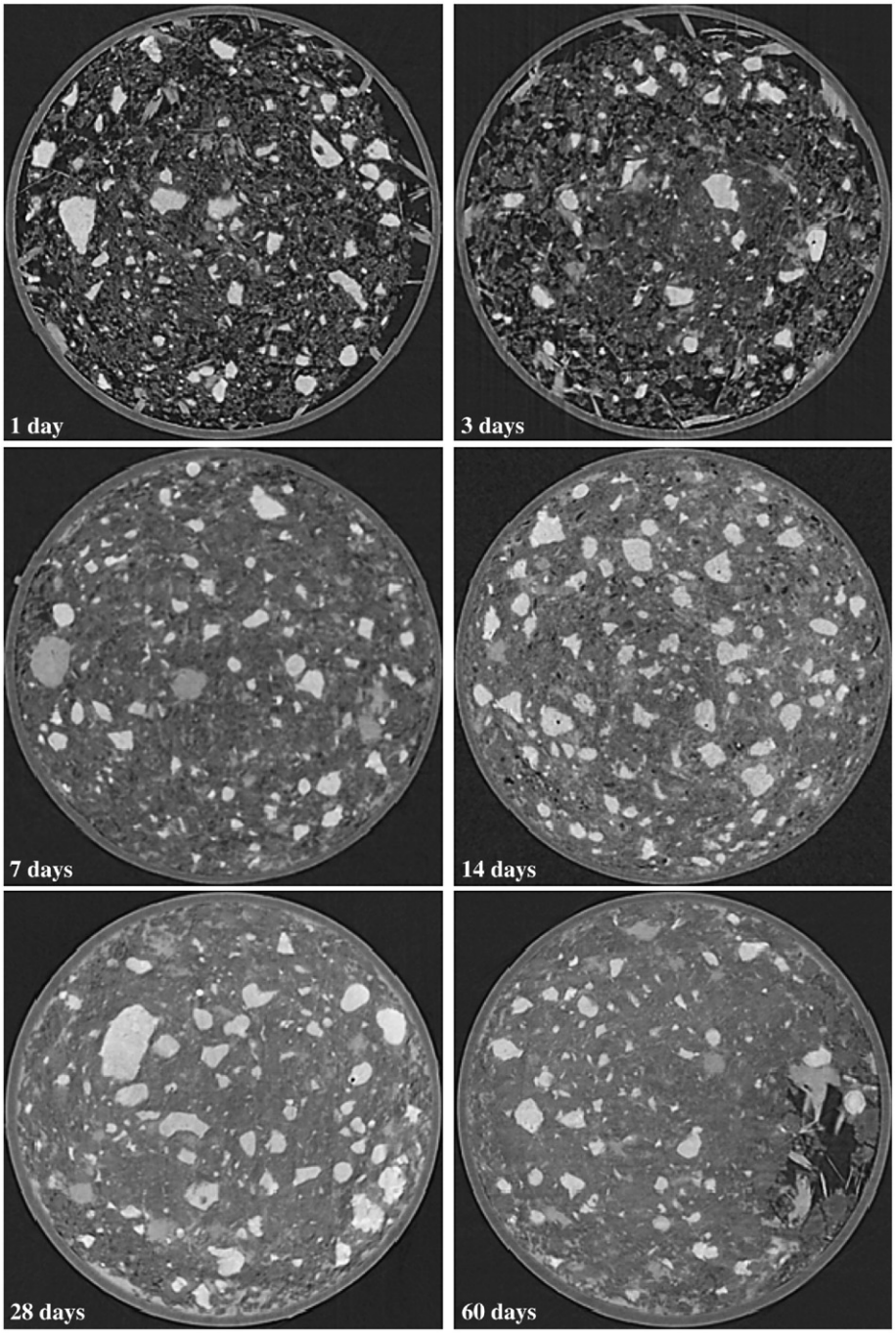

Fig. 3. Evolution of the microstructure with hydration time (series 1).

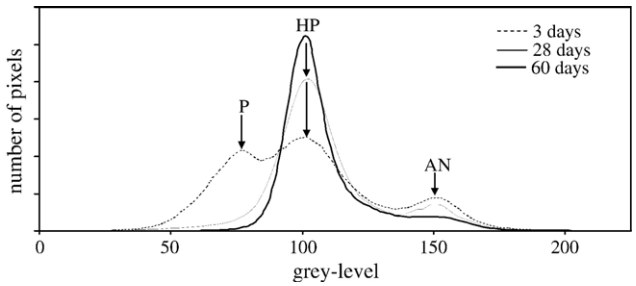

Fig. 4. Phases evolution through gray-level histogram of slices.

using different samples for the various ages instead of observing a single sample over 60 days is that since it is very difficult to achieve a homogeneous and reproducible filling of the tubes due to their small cross section, some variations in the results correspond to variations between samples.

A second series of experiments (series 2) was then conducted in order to prevent the variations due to sample preparation: the same capillary was studied over time between 1 and 60 days. This necessitated access to the synchrotron beam line at the required ages of the sample. Between two tomographic acquisitions, the capillary was kept unsealed in distilled water. Results from both series are presented and compared.

2.2. Synchrotron measurement and back projection reconstructions

Tomographic scans were performed at the Swiss Light Source (SLS) in Villigen (Switzerland) on the MS-X04SA-Tomo beam line [14]. Depending on the sample age, the beam energy was set to values from 12.3 to 15 keV, the intensity being kept constant at 200 mA. 1001 projections with an angle step of 0.18° and an exposure time of 3 s each were acquired on a 2048px CCD camera equipped with a 1400 mm field of view and a 10× magnification optical objective. The pixel resolution under these conditions was 0.6835 μm. Reconstructed slices (tomograms) were computed using the Filtered Back Projection algorithms [15] in use at the SLS. It should be noted that there was no prior drying or other preparation of the sample before imaging. The short exposure times and configuration of the line ensure that there is no significant heating or drying of the sample during the acquisition of the images.

3. Results and discussion

3.1. Qualitative analysis of the reconstructed slices

Fig. 2(1) shows a raw reconstructed slice of a 1 day old sample. From a qualitative point of view, the resolution of these computed images is comparable to that usually observed using scanning electron microscopy at an equivalent magnification (Fig. 2(3)). Though the beam–matter interactions are fundamentally different, the X-ray projections and SEM backscattered electron mode lead to similar phase contrast:

- unreacted anhydrous cement grains (labeled A in Fig. 2) are the brightest phases in both modes (more BSE emitted in the SEM and more X-rays absorbed with the synchrotron) as they have the highest density.
- 'inner' C-S-H (rims around anhydrous grains) and undifferentiated hydration products (hydrates filling the cementitious matrix) are grey (labeled B).
- calcium hydroxide, CH (labeled C) is light grey (slightly darker than anhydrous grains).
- porosity (labeled D) appears as the darkest phase (no interaction with either beam).

Besides the access to the third dimension, the interest of tomography, compared to SEM–BSE images, is that no prior preparation of the paste — drying, resin impregnation and polishing are needed. Therefore any possible artefacts are avoided. The high degree of similarity between the two images thus provides direct evidence that alterations in microstructure produced by preparation for SEM are minimal at the resolution of the technique.

At present the resolution of the tomographic technique is limited by the resolution of the camera. However as all the images are acquired through the whole thickness of the sample, the quality of the filters used in the reconstruction process also plays an important role in the quality of the image obtained. The reliability of the SLS setup and the quality of the Filtered Back Projection algorithms allow a good discrimination of the solid phases, for instance the resolution of intermixed CH clusters and outer C-S-H in the centre of the slice in Fig. 2.

Fig. 3 illustrate the evolution of the microstructure during the hydration reaction. As the age of the samples increases, the anhydrous cement reacts to give hydrated phases (C-S-H and CH) which fill the pores. This is clearly seen both in the slices and in the corresponding grey level histograms (Fig. 4) in which the area of the peak corresponding to anhydrous cement (AN) decreases significantly, while that of the hydration products (HP) increases. At 3 days, the amount of pores is high enough to generate a peak in the histogram. Since the grey levels of HP and pores are close to each other, the frontier between the two peaks is not well delimited so that they overlap. At 28 days, the pore content has decreased and a separate peak is no longer observed. However, in the grey level range previously identified as porosity there are still pixels, meaning that some porosity is still detectable. At 60 days, no porosity can be detected i.e. pores were refined up to the point of being smaller than the resolution of the method. The decrease of the size of pores from

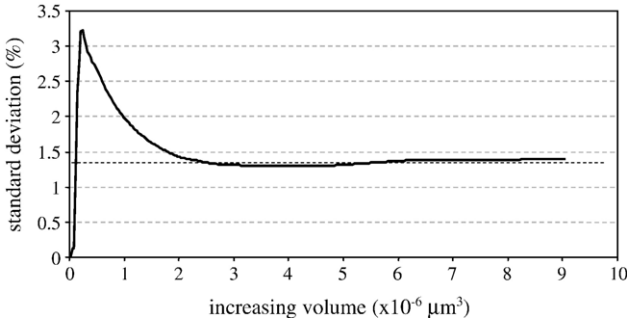

Fig. 5. Stabilisation of the standard deviation of the porosity mean in a 1 day sample vs increasing ROI (300 slices ≈ 200 μm).

28 to 60 days can however be appreciated thanks to the sharpening of the left edge of the HP peak: since fine capillary pores are intermixed with hydration products they contribute to the HP average grey level. The sharpening of the HP peak at 60 days means that less or smaller pores are intermixed with the C-S-H matrix.

On the basis of the above qualitative observations, the slices obtained using tomography, at least at an early age, can thus be considered as suitable as BSE images for phase discrimination at the same resolution.

These images also illustrate the difficulty to achieve a homogeneous filling of the capillary tube: in some samples the compactness of the paste decreases from the centre towards the tube walls whereas others are more homogeneous. This indicates the problems of reproducibility of the samples and obviously puts into question the exact water to cement ratio of each sample. As mentioned previously, this problem has then been partly solved by using one single sample over 60 days (series 2).

3.2. Extraction of quantitative data

This section illustrates the suitability of μCT to quantitatively study microstructural parameters concerning both solid phases (i.e. unreacted cement grains) and the pore network. To reduce the computing time and to avoid edge effects, the study was limited to a region of interest (ROI) of volume of 8×10^6 μm^3 (cube with an edge of 200 μm i.e. 300 slices) taken in the centre of the slices where the paste is the most homogeneous. To check that this volume was statistically representative, the standard deviation of the considered features in a series of volumes of progressively large sizes was measured (for instance, pore content in Fig. 5). This indicates that the ROI chosen is well above the size at which the fluctuation between different volumes becomes steady.

3.2.1. Image processing

In order to maintain as much of the information in the images as possible, very little image processing was performed: only a three dimensional median filter ($3 \times 3 \times 3$ voxels) was applied to the whole stack of reconstructed slices in order to even out brightness and contrast variations between successive slices. Unreacted cement grains and porosity were isolated by thresholding the slices on the basis of their grey level histograms. As the difference in absorption coefficients between air and water is below the resolution of the technique [12], both air voids and free water contribute to the porosity peak. No distinction between the two contributions was therefore made.

3.2.2. Reactivity of anhydrous cement grains

Fig. 6 shows the reconstructed volume of a 1 day old sample as well as the corresponding segmented anhydrous (unreacted cement) fraction (AN). From such images the easiest data to extract is the evolution of the total amount of AN with time (Fig. 7(a). When the water to cement ratio is known, this can be converted into the degree of hydration. In Fig. 7(b), a water to cement ratio of 0.5

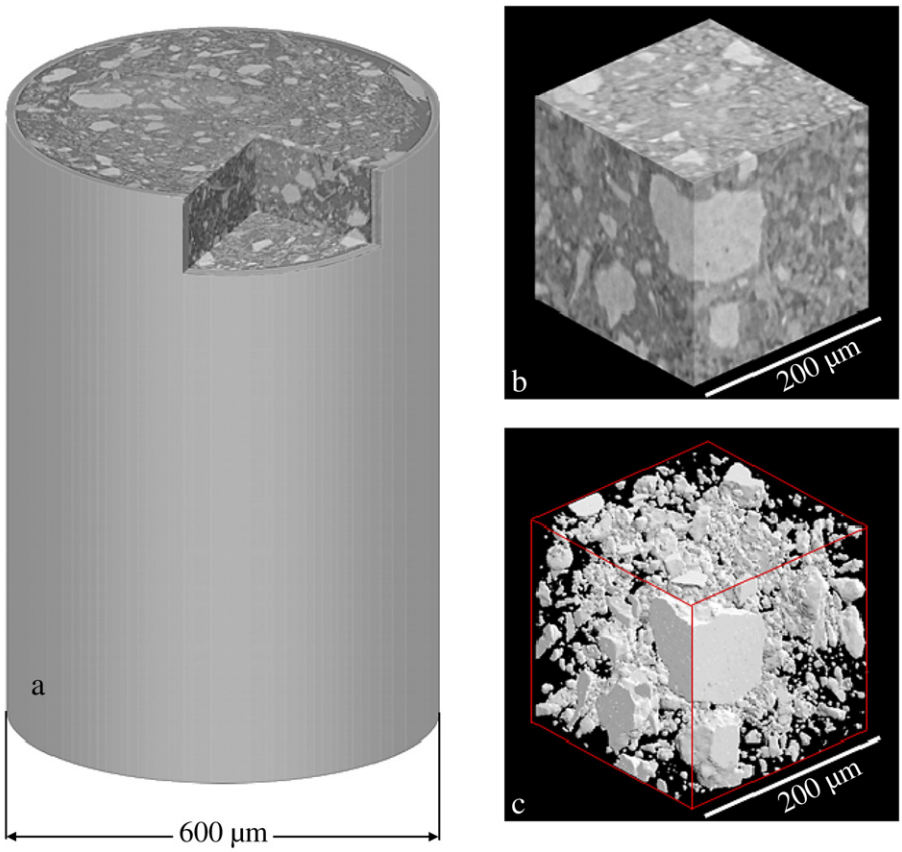

Fig. 6. 3 days old reconstructed sample (a), volume of interest (b) and segmented cement fraction (c).

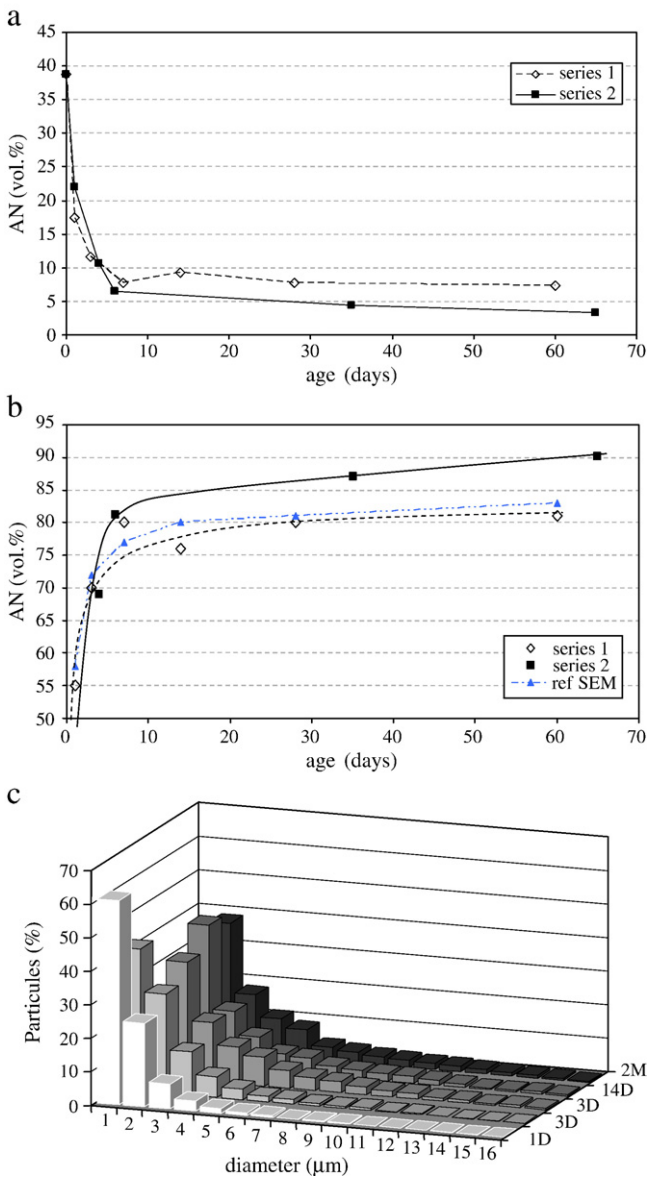

Fig. 7. Unreacted cement content (a), hydration degree assuming a W/C ratio of 0.5 (b) and relative AN particle size distribution evolution with time for series 1 (c).

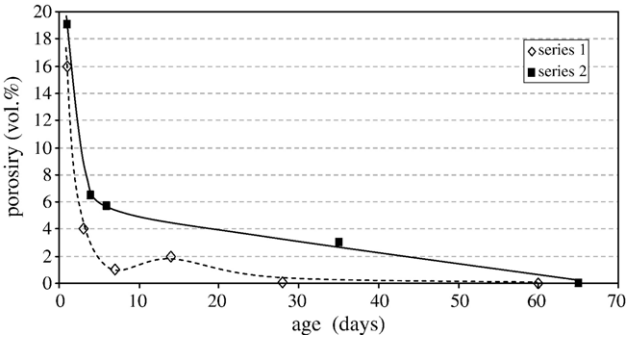

Fig. 9. Volume content of pores.

was used for the calculations. The divergence between the two series is almost certainly related to a difference in their actual W/C. The figure also shows data obtained from an SEM study, where good control of W/C is possible [16]. The data in series 1, lies along the same trend, but shows considerable fluctuations, due to the fact that a separate sample was used for each measurement. The series 2 data show a better monotonic progression, but differ systematically from the SEM data due to the different W/C of the one sample studied in this series. Assuming that the rate of hydration be similar in all cases, the over estimate of the degree of hydration for series 2 arises from the fact that the W/C of this series was higher than 0.5.

Beyond averaged quantitative measurements, the real strength of microtomography is that it offers ways to study 3D features. For instance, rather than the overall AN content, Fig. 7(c) gives the evolution of AN particle size distribution during hydration. This is a direct measure of the volume distribution in three dimensions, without the need to make an unfolding analysis of measures in 2D, with the incumbent problems of assumption of particle shape and the statistical uncertainty for the small particles [17,18]. The results are consistent with expectations: as hydration progresses, small grains are rapidly consumed so that their relative amount decreases compares to the total number of grains. Various other 3D properties could also be measured (for instance, mean path between specific features) without any statistical extrapolation of 2D data. Such 3D analysis of this data was not made in this study, due to the sample heterogeneities and unknown exact W/C ratio as described above.

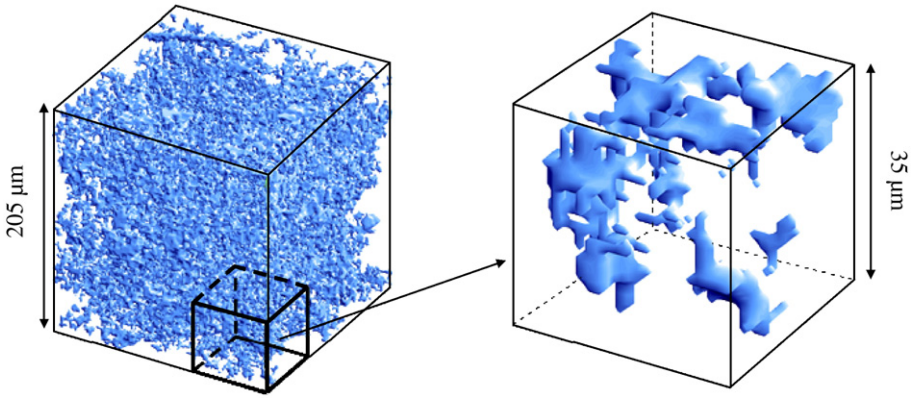

Fig. 8. Pore network segmentation of a 3 days old paste (series 1).

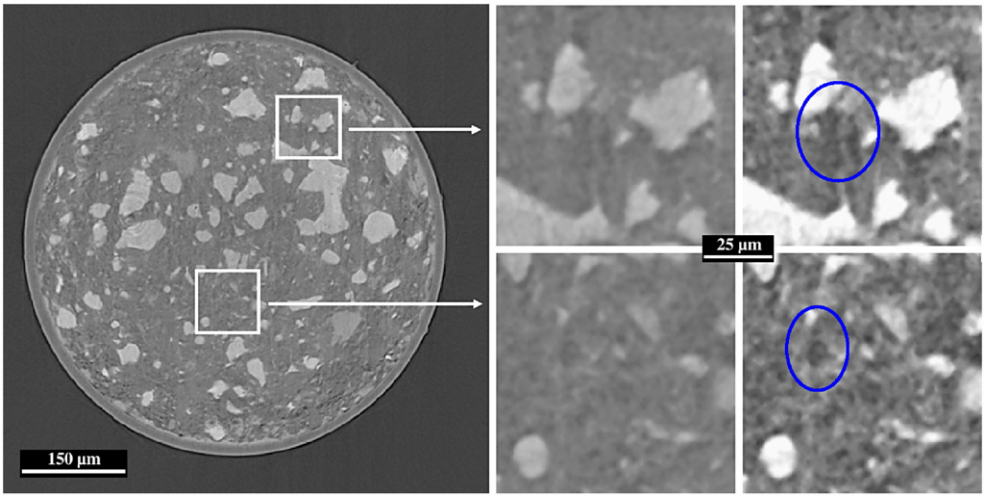

Fig. 10. Loss of contrast on pores due to their change in attenuation coefficient with time. centre— zoom on squared areas in left image right— contrast enhancement of (b): darkest areas (in circles) are often partially filled with hydrated products; an average attenuation coefficient corresponding to (void+product) is generated and the two 'phases' cannot be discriminated realistically.

3.2.3. Porosity

A region growing algorithm was used to isolate the porosity of the pastes from the bulk. Such an algorithm scans the image until it finds a pixel (called a seed) in the range of threshold values and then searches for all pixels connected to this seed within the threshold limits. When all connected pixels have been found, the algorithm looks for another seed. This segmentation method is more efficient to preserve the connectivity of a phase (which makes sense for porosity) than a simple grey level threshold. Fig. 8 illustrates the result obtained for a 3 days old sample. This is the first time that an experimental technique allows the visualisation and investigation of the complete 3D pore network. From a qualitative point of view, the magnified part in Fig. 8 clearly shows the connectivity and tortuosity of such a network. Of course the resolution, of just below 1 µm, is still comparatively large relative to the typical sizes of the capillary porosity, nevertheless for the young pastes these images provide much information.

Two distinct kinds of quantitative information can be extracted from these data: the first concerns global parameters (overall volume, specific surface, size distribution…) while the second, morphological or local parameters (topology, connectivity…).

Fig. 9 gives the evolution of the total porosity and as a function of time. The general trend of the curves is as expected; the average radius of pores decreases over time until the network is only made of very fine pores. As the resolution is limited to 0.7 µm, fewer and fewer pores are detected as they become finer so that their total volume tends to 0. The trend differs between the two samples because of the differences in W/C, supporting the conclusion that the series 2 has a higher W/C ratio.

However, although the pore network of cementitious materials is expected to decrease with time, such low levels as those measured here are rather unusual and SEM images clearly show that micron sized pores are usually observed at ages greater than 60 days. A closer examination of tomographic sections reveals that pores are still present under the form of isolated groups of dark pixels but with a grey level very closed to that of HP (Fig. 10). This loss in contrast resolution seems to increase with the decrease of pore size, especially when it approaches the spatial resolution limit of the technique. The contrast is defined here by the difference in attenuation between the feature and the background, divided by the background attenuation; the ability to discriminate between two phases with close linear attenuation values will thus depend

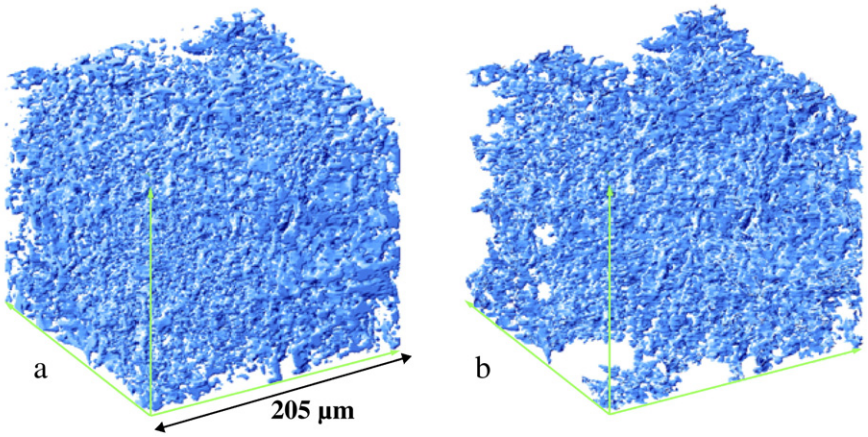

Fig. 11. Total porosity (a) and percolating pore network (b) of a 3 days old paste (series1).

on the accuracy with which their attenuation can be measured [19]. Therefore, the X-rays need to be sufficiently energetic to penetrate the sample such that adequate counting statistics can be obtained; but on the other hand, if the source is too powerful, the difference in attenuation will be low and the object becomes virtually transparent, with little or no contrast between the phases. In the present case, since the empty space is progressively filled with C-S-H while porosity is decreasing, the contrast resolution is lost when pores reach the spatial resolution limit.

This explains why lower porosity values are obtained than from BSE images in the SEM (in which the phase contrast generation is completely different). However, during the first days of hydration, the reliability of the results makes synchrotron X-ray tomography the most relevant technique for the 3D investigation of the pore network of cementitious materials.

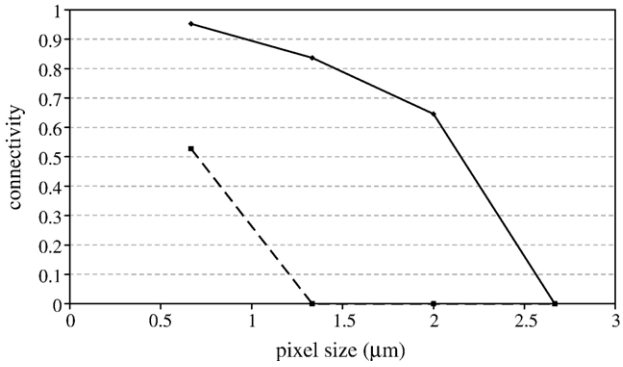

Fig. 13. Dependence of the connectivity degree with the spatial resolution.

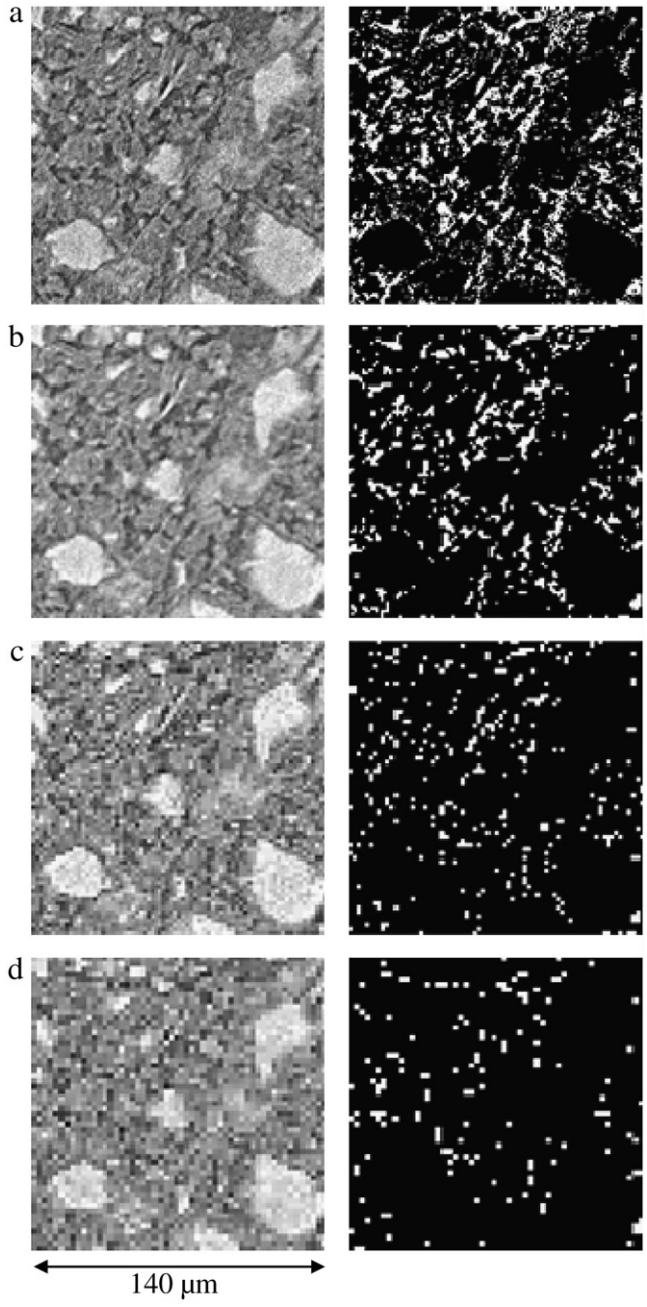

Fig. 12. Porosity content as a function of pixel size. a—(0.67 μm, 18.60%) b—(1.34 μm, 11.48%) c—(2 μm, 6.63%) d—(2.67 μm, 5.03%).

As for solid phases, the strength of the microtomography approach lies in the possibility to characterise 3D morphological parameters: Fig. 11(b) shows the connected fraction of the whole pore network represented in Fig. 11(a). This connected network has links to all faces of the considered VOI. It means that any external species entering from one face can progress to any other face. From these experimental images, it is observed that at 1 and 3 days, there is a high degree of percolation of the porosity through the solid materials. After 7 days, the pore network does not percolate any longer at this scale since the content of pores is very low and highly disconnected.

The influence of the resolution on the percolation of porosity in microstructural models has been discussed by Garboczi et al.[20] and Pignat et al.[21]. Using their respective models, both teams have calculated that increasing the pixel size decreases the calculated connectivity of phases. The effect of pixel size on the porosity of a randomly chosen section was experimentally assessed and is shown in Fig. 12. From top to bottom, upon decreasing the resolution four times, the detected porosity of the same unit respectively goes from 18.60% to 5.03%. Obviously, this has a large impact on the calculated percolation of the pore network; decreasing its connectivity. Fig. 13 shows the calculated connectivity as a function of the pixel resolution, for the 1 day and 3 day images. It is observed that at 1 day, the pore network is large enough to still percolate when the resolution decreases, while at 3 days, maximum pore resolution is already close to the percolation limit. Of course the percolation limit applies at the, relatively large, resolution of the images (around 1 μm) and it is probable that the capillary porosity of these samples still percolates at a lower scale.

4. Conclusions

The results obtained in this study clearly show the suitability of synchrotron microtomography as a non invasive technique for the three dimensional investigation of cementitious materials. The qualitative and quantitative information accessible can make a major contribution to the study of the microstructural development of cementitious materials. The main interest is certainly the access to the real pore network that forms and its evolution with time.

Both geometrical and morphological parameters can be quantified, which makes this a valuable technique for the study of cementitious materials.

The main drawback of this method is its spatial resolution which is at present quite low relative to the sizes of capillary pores controlling transport properties in mature pastes. The resolution is further limited by the relatively similar attenuation coefficients of pores and C-S-H relative to unreacted cement, which makes the pores hard to resolve when their size reaches the spatial resolution of the technique. Nevertheless in the early stages of hydration the information can be interfaced with microstructural models, which in turn should allow extrapolation to higher degrees of hydration and longer ages. Furthermore, technological improvements should allow improved resolution in the future as the theoretical limit has not yet been reached.

Another problem encountered here concerns sample preparation since it is very difficult to control the homogeneity and water to cement ratio in the very fine capillary tubes used here. However, the resolution of fine pores is only possible when the overall sample size is also small. For larger samples there would be lower transmission of X-rays therefore more attenuation problems as well as much longer acquisition times.

Despite these limitations, the technique has several advantages: first, it is the only non invasive imaging technique available so far, which means that all phenomena associated with the development of the hydration can be studied 'in situ'. Second, the access to the third dimension is a plus as new features such as connectivity can be studied.

References

[1] M.K. Head, H.S. Wong, N.R. Buenfeld, Characterisation of 'Hadley' grains by confocal microscopy, Cement and Concrete Research 36 (8) (2006) 1483–1489.

[2] K.L. Scrivener, Backscattered electron imaging of cementitious microstructures: understanding and quantification, Cement and Concrete Composites 26 (8) (2004) 935–945.

[3] B. Flannery, H. Deckman, W. Roberge, K. D'Amico, Three-dimensional X-ray microtomography, Science 237 (1987) 1439–1443.

[4] C. Hall, S.L. Colston, A.C. Jupe, S.D.M. Jacques, R. Livingston, A.O.A. Ramadan, A.W. Made, P. Barnes, Non destructive tomographic energy dispersive diffraction imaging of the interior of bulk concrete, Cement and Concrete Research 30 (3) (2000) 491–495.

[5] T.J. Chotard, M.P. Boncoeur-Martel, A. Smith, J.P. Dupuy, C. Gault, Application of X-ray computed tomography to characterise the early hydration of calcium aluminate cement, Cement and Concrete Composites 25 (2003) 145–152.

[6] F.M. Auzerais, J. Dunsmuir, B.B. Ferreol, N. Martys, J. Olson, T.S. Ramakrishnan, D.H. Rothman, L.M. Schwartz, Transport in sandstone: a study based on three-dimensional microtomography, Geophysical Research Letters 23 (7) (1996) 705–708.

[7] E. Rosenberg, J. Lynch, P. Gueroult, M. Bisiaux, R. Ferreira De Paiva, High resolution 3D reconstructions of rocks and composites, Oil & Gas Science and Technology— Review 54 (4) (1999) 497–511.

[8] D.P. Bentz, N.S. Martys, P.E. Stutzman, M.S. Levenson, E.J. Garboczi, J. Dunsmuir, L.M. Schwartz, X-ray microtomography of an ASTM C109 mortar exposed to sulfate attack, MRS Symposium Proceedings, vol. 370, 1995, pp. 77–82.

[9] E.N. Landis, A.L. Petrell, S. Lu, E.N. Nagy, Examination of pore structure using three-dimensional image analysis of microtomographic data, Concrete Science and Engineering 2 (2000) 162–169.

[10] D.P. Bentz, S. Mizell, S. Satterfield, J. Devaney, W. George, P. Ketcham, J. Graham, J. Porterfield, D. Quenard, F. Vallee, H. Sallee, E. Boller, J. Baruchel, The visible cement data set, Journal of Research of the National Institute of Standards and Technology 107 (2002) 137–148.

[11] D.P. Bentz, D.A. Quenard, H.M. Kunzel, J. Baruchel, F. Peyrin, N.S. Martys, E.J. Garboczi, Microstructure and transport properties of porous building materials. II: three-dimensional X-ray tomographic studies, Materials and Structures 33 (2000) 147–153.

[12] L. Helfen, F. Dehn, P. Mikulik, T. Baumbach, Synchrotron radiation X-ray tomography : a method for the 3D verification of cement microstructure and its evolution during hydration, Proceeding 'First International Congress on Nanotechnologies in the Construction Industry', Glasgow, June 2003.

[13] K.L. Scrivener, A.K. Crumbie, P. Laugesen, The Interfacial Transition Zone (ITZ) between cement paste and aggregate in concrete, Interface Science 12 (4) (2004) 411–421.

[14] M. Stampanoni, G. Borchert, P. Wyss, R. Abela, B. Patterson, S. Hunt, D. Vermeulen, P. Rüegsegger, Nuclear Instruments and Methods in Physics Research, A 491 (2002) 291–301.

[15] R.H. Huesman, G.T. Gullberg, W.L. Greenberg, T.F. Budinger, Donner Algorithms for Reconstruction Tomography, Publication PUB-214, Lawrence Berkeley Laboratory, 1977.

[16] K.L. Scrivener, T. Füllmann, E. Gallucci, G. Walenta, E. Bermjo, Quantitative study of Portland cement hydration by X-ray diffraction/Rietveld analysis and independent methods, Cement and Concrete Research 34-9 (2004) 1541–1548.

[17] T. Allen, Particle Size Measurements, volume 1, Ed. Chapman et Hall, 1997, 5th ed.

[18] K.L. Scrivener, Microscopy methods in cement and concrete science, World Cement Research and Development, September 1997, pp. 92–112.

[19] D. Wildenschild, C.M.P. Vaz, M.L. Rivers, D. Rikard, B.S.B. Christensen, Using X-ray computed tomography in hydrology: systems, resolutions, and limitations, Journal of Hydrology 267 (3–4) (2002) 285–297.

[20] E.J. Garboczi, D.P. Bentz, The effect of statistical fluctuation, finite size error, and digital resolution on the phase percolation and transport properties of the NIST cement hydration model, Cement and Concrete Research 31 (10) (2001) 1501–1514.

[21] C. Pignat, P. Navi, Simulation of cement hydration and the connectivity of the capillary pore space, Advanced Cement Based Materials 4 (2) (1996) 58–67.